Development 138, 565-575 (2011) doi:10.1242/dev.056903

PDGF-A controls mesoderm cell orientation and radial intercalation during *Xenopus* gastrulation

Erich W. Damm and Rudolf Winklbauer*

SUMMARY

Radial intercalation is a common, yet poorly understood, morphogenetic process in the developing embryo. By analyzing cell rearrangement in the prechordal mesoderm during *Xenopus* gastrulation, we have identified a mechanism for radial intercalation. It involves cell orientation in response to a long-range signal mediated by platelet-derived growth factor (PDGF-A) and directional intercellular migration. When PDGF-A signaling is inhibited, prechordal mesoderm cells fail to orient towards the ectoderm, the endogenous source of PDGF-A, and no longer migrate towards it. Consequently, the prechordal mesoderm fails to spread during gastrulation. Orientation and directional migration can be rescued specifically by the expression of a short splicing isoform of PDGF-A, but not by a long matrix-binding isoform, consistent with a requirement for long-range signaling.

KEY WORDS: Gastrulation, PDGF-A, Intercalation, *Xenopus*, Cell migration

INTRODUCTION

Radial intercalation is a basic morphogenetic process. In early development, it is essential for the large-scale rearrangements of embryonic parts involved in gastrulation. For example, the upper half of the amphibian blastula consists of prospective ectoderm, whereas the mesoderm forms a narrow ring below the equator. During gastrulation, these regions expand to eventually cover the endodermal core of the embryo (Fig. 1A,B). In the absence of growth, expansion occurs by a respective thinning of these two germ layers, brought about mainly by an interdigitation of cells in the radial direction, i.e. by radial intercalation (Keller et al., 2003).

In the *Xenopus* embryo, radial intercalation underlies the spreading of the inner ectodermal layer during epiboly (Keller, 1980; Marsden and DeSimone, 2001). In the chordamesoderm, it cooperates with mediolateral cell intercalation to promote convergent extension (Wilson and Keller, 1991; Keller, 2002), and it occurs also in prechordal, lateral and ventral mesoderm (Keller and Tibbetts, 1989; Winklbauer and Schurfeld, 1999; Ibrahim and Winklbauer, 2001). Despite its ubiquity, however, radial intercalation is not well understood at the cellular level, and its molecular control is virtually unknown. Thus, in the mesoderm, radial intercalation is an active process (Wilson and Keller, 1991; Winklbauer and Schurfeld, 1999; Ibrahim and Winklbauer, 2001), but neither the polarity and orientation of the interdigitating cells, nor the orienting cues have been determined.

We show here that radial intercalation in the prechordal mesoderm (PCM), i.e. in the region where thinning of the mesoderm layer is greatest (Fig. 1B,C), is driven by an attraction of its cells to the blastocoel roof (BCR) by platelet-derived growth factor (PDGF). The PDGF family contains four members, PDGF-A, -B, -C and -D, which are recognized by two receptor tyrosine kinases, PDGFR-α and PDGFR-β (Andrae et al., 2008). In many vertebrate gastrulae, including *Xenopus*, PDGF-A and PDGFR-α are expressed in a complementary fashion, with the ligand in the ectoderm and the receptor in the mesoderm (Ataliotis et al., 1995; Orr-Urtreger and Lonai, 1992; Yang et al., 2008).

Two PDGF-A isoforms are generated by alternative splicing. The long form (lf-PDGF-A) contains a matrix-binding motif of positively charged amino acid residues that interacts with cell surface and extracellular components such as heparin sulfate proteoglycans (Smith et al., 2009; Andersson et al., 1994; Raines and Ross, 1992). In the *Xenopus* gastrula, lf-PDGF-A is deposited in the BCR extracellular matrix to guide mesoderm migration on the BCR towards the animal pole (Nagel et al., 2004; Smith et al., 2009). The short, diffusible isoform (sf-PDGF-A) lacks the matrix-binding motif (Andrae et al., 2008; Mercola et al., 1988; Raines and Ross, 1992). To our knowledge, no specific developmental role has been assigned yet to sf-PDGF-A.

We show that sf-PDGF-A acts as a long-range signal to orient and attract the cells of the multilayered PCM towards the BCR, leading to radial intercalation. This establishes a dual role for PDGF-A, based on differential splicing, where the long form regulates directional mesoderm migration across the BCR surface (Nagel et al., 2004) and the short form radial intercalation of the deep PCM cells. Furthermore, it provides for the first time insight into the molecular basis of a radial intercalation movement in the vertebrate gastrula.

MATERIALS AND METHODS

Embryos and microinjections

Xenopus laevis embryos were fertilized as described previously (Luu et al., 2008), and staged according to Nieuwkoop and Faber (Nieuwkoop and Faber, 1967). Embryos were microinjected in 4% Ficoll solution with mRNA or morpholino oligonucleotides (MO) (GeneTools) at the four-cell stage in either the animal (BCR expression), dorsal marginal (mesoderm expression) or vegetal region (endoderm expression), and kept in 1/10× Modified Barth's solution (MBS) at 15°C until the required stage.

Explants

For slice explants, slices of dorsal mesoderm and attached endoderm were combined with inner ectoderm from the animal BCR (Fig. 5A). For mesoderm-ectoderm or mesoderm-endoderm combined explants, PCM, inner cells from the animal region of the BCR, or endoderm from the vegetal cell mass were dissected, combined and secured under a strip of

Department of Cell and Systems Biology, University of Toronto, 25 Harbord Street, Toronto, Ontario, M5S 3G5, Canada.

*Author for correspondence (r.winklbauer@utoronto.ca)

Accepted 23 November 2010

coverslip, with the mesoderm side originally in contact with the BCR facing down, and the BCR explant positioned opposite to the endogenous leading edge (Fig. 6A). Explants were kept in 1× MBS on 1% BSA treated glass bottom dishes (MatTek). Explants were filmed for 90 minutes using a Zeiss Axiovert 200 M inverted microscope.

Scanning electron microscopy

Embryos were fixed in 2.5% glutaraldehyde/0.1 M sodium cacodylate overnight at 4°C, post-fixed in osmium tetraoxide, and treated with an ethanol/0.1 M cacodylate and ethanol/hexamethyldisilizane dehydration series. Specimens were dried overnight and sputter coated with gold-palladium.

mRNA isolation and RT-PCR

PCM, endoderm and animal caps were dissected at stages 11 and 12. RNA was purified (TriZol, Invitrogen) and cDNA was synthesized (Superscript III, Invitrogen). The following primers were used for PCR reactions: PDGF-A (long/short form), FWD 5′-GGAATGCACGTGTACAGCAA-3′ and REV 5′-CGGGAATGTAACATGGCGTA-3′; PDGFR-α, FWD 5′-CTCGCAAATGCCACTACAGA-3′ and REV 5′-CCACAAGGTGT-CATTGTTGC-3′; ODC, FWD 5′-GTCAATGATGGAGTGTATGGATC-3′ and REV 5′-TCCATTCCGCTCTCCTGAGCAC-3′; Gsc, FWD 5′-TGTGGAGCAGTTCAAGCTCT-3′ and REV 5′-ATCTGGGTACTTG-GTTTCTT-3′; and xBra, FWD 5′-GGATCGTTATCACCTCTG-3′ and REV 5′-GTGTAGTCTGTAGCAGCA-3′. Reactions for PDGF-A/PDGFR-α and ODC were run for 30 and 23 cycles, respectively, at an annealing temperature of 60°C, reactions for Gsc and xBra for 25 cycles at an annealing temperature of 55°C.

Constructs, morpholinos and mRNA synthesis

RNA was synthesized using mMessage mMachine kits (Ambion). Plasmids containing lfPDGF-A (pGHE2), sfPDGF-A (pCS2+), PDGFR-α (pGHE2), PDGFR-37 (pGHE2) and dnPDGF-A 1308 (pGEM) were prepared for transcription as described by Nagel et al. (Nagel et al., 2004). PDGF-A morpholino (5′-AGAATCCAAGCCCAGATCCTCATTG-3′) was used as described previously (Nagel et al., 2004). Morpholino-resistant variants of sf/lf-PDGF-A were generated using the QuickChange II site-directed mutagenesis kit (Stratagene). Five bases (A, G, C, T, T) within the morpholino hybridization region, were changed (to C, A, T, C, A, respectively). Sense (5′-GCAGCAGGACGCAATGCGAATTTGGG-CCTGGATACTGCTGCTAAGCGTCG-3′) and antisense (5′-AGACGC-TTAGCAGCAGTATCCAGGCCCAAATTCGCATTGCGTCCTGCT-GC-3′) primers were used. Amino acid composition of the protein was preserved.

In situ hybridization

In situ hybridization was performed according to Harland (Harland, 1991). Antisense mRNA probes for Xbra, Gsc and Cer were generated according to Nagel et al. (Nagel et al., 2004); the Cer plasmid was linearized with *Eco*RI. mMessage mMachine kit (Ambion) NTPs were substituted with DIG-labeled NTPs (Roche). Anti-DIG alkaline phosphatase conjugated antibodies (Roche) were used for detection. BM Purple (Roche) was the substrate for alkaline phosphatase.

Statistical analysis

Statistical analysis was performed using GraphPad inStat 3. The Mann-Whitney statistical test at the 95% confidence level was used for all statistical calculations.

RESULTS

Prechordal mesoderm cells are oriented toward the BCR and intercalate radially

To analyze the arrangement of its cells, the dorsal mesoderm was divided into three regions. Expression of *Xenopus brachyury* (*Xbra*) demarcates the chordamesoderm, and *goosecoid* (*gsc*) the PCM (Fig. 1D,F″-G″) (Wilkinson et al., 1990; Cho et al., 1991). The leading edge mesendoderm (LEM) was defined as the region between the anterior boundary of *gsc* expression and the leading edge (Fig. 1D,E); it expresses *cerberus* (*cer*) (Fig. 1E-E″) (Bouwmeester et al., 1996). In order to determine the extent of the *xBra* and *gsc* regions on SEM micrographs, the length and width of these expression domains relative to total mesoderm size was determined from images of in situ hybridization experiments (see Fig. S1 in the supplementary material).

In the LEM, cell shapes and sizes varied, but all cells exhibited a distinct polarity with a single protrusion-bearing pole. Cells were oriented obliquely with respect to the BCR (Fig. 1E,J), and attached their lamelliform protrusions to neighboring cells (Fig. 1E). When viewed from the substrate side, this orientation appears as a shingle arrangement of cells (Fig. 1E′) (Nagel et al., 2004; Winklbauer and Nagel, 1991).

Cells of the PCM were elongated perpendicular to the BCR (Fig. 1F,I), and were unipolar, with a protrusion-bearing front end pointing towards the BCR, and a rounded rear (Fig. 1F; see Fig. S2A-F in the supplementary material). Protrusions were lamelliform or filiform, and appeared attached to neighboring cells (Fig. 1F; see Fig. S2A-F in the supplementary material). When the BCR was removed, protrusions formerly in contact with the BCR did not exhibit any obvious orientation (Fig. 1F′).

The *Xbra*-expressing blastopore lip is the site of involution. Its chordamesoderm cells extended multiple lamelliform and filiform protrusions (Fig. 1G). When the lip was fractured parallel to the embryo surface, mediolaterally oriented bipolar cells were visible (Fig. 1G′), consistent with mediolateral cell intercalation (Keller and Tibbetts, 1989; Shih and Keller, 1992). Internalized chordamesoderm cells directly above the lip region were oriented with their long axes perpendicular to the BCR (Fig. 1G). However, although PCM cell protrusions are all directed towards the BCR, chordamesoderm protrusions pointed either towards or away from the BCR, at this or at later stages (Fig. 2H,H′; see Fig. S2G,H in the supplementary material), while cells remained unipolar (Fig. 2H,H′; see Fig. S2G,H in the supplementary material). This suggests that the radial orientation of chordamesoderm cells is regulated differently from that of PCM cells.

To quantify cell orientation, the angles at which protrusions extended relative to the BCR were measured (Fig. 1H). Throughout mid-gastrulation, PCM cells were highly oriented toward the BCR (Fig. 1I). LEM cells mostly extended protrusions at angles between 0 and 70 degrees (Fig. 1J). The transition from perpendicular to oblique orientation was gradual (Fig. 1D, white box). The long axes of the large endodermal cells located deep to the PCM were oriented in parallel to the BCR (Fig. 1K), but polarity could not be determined in the absence of distinct protrusions.

We also determined the positions of PCM protrusions relative to anterior/posterior or lateral neighbors. We found that PCM cells extend protrusions between neighboring cells in any anteroposterior or mediolateral plane, and no correlation with the direction of overall mesoderm translocation on the BCR was apparent (see Fig. S3A-C in the supplementary material). Some cells extended multiple lamelliform protrusions from a single pole of the cell in two planes simultaneously (see Fig. S2D-F in the supplementary material).

Comparison of PCM thickness at mid- and late-gastrula stages showed a distinct thinning (Fig. 2A). To determine whether this is due to a rearrangement or a flattening of cells, we measured the layer index, i.e. tissue thickness in terms of cell layers (Keller, 1980) (see Fig. S2I in the supplementary material). It changed little between stages 10.5 and 11, but during the 2-hour period between stages 11 and 12 it decreased from 2.5 to 1 (Fig. 1F, Fig. 2B). Together with the presence of oriented protrusions, this suggests

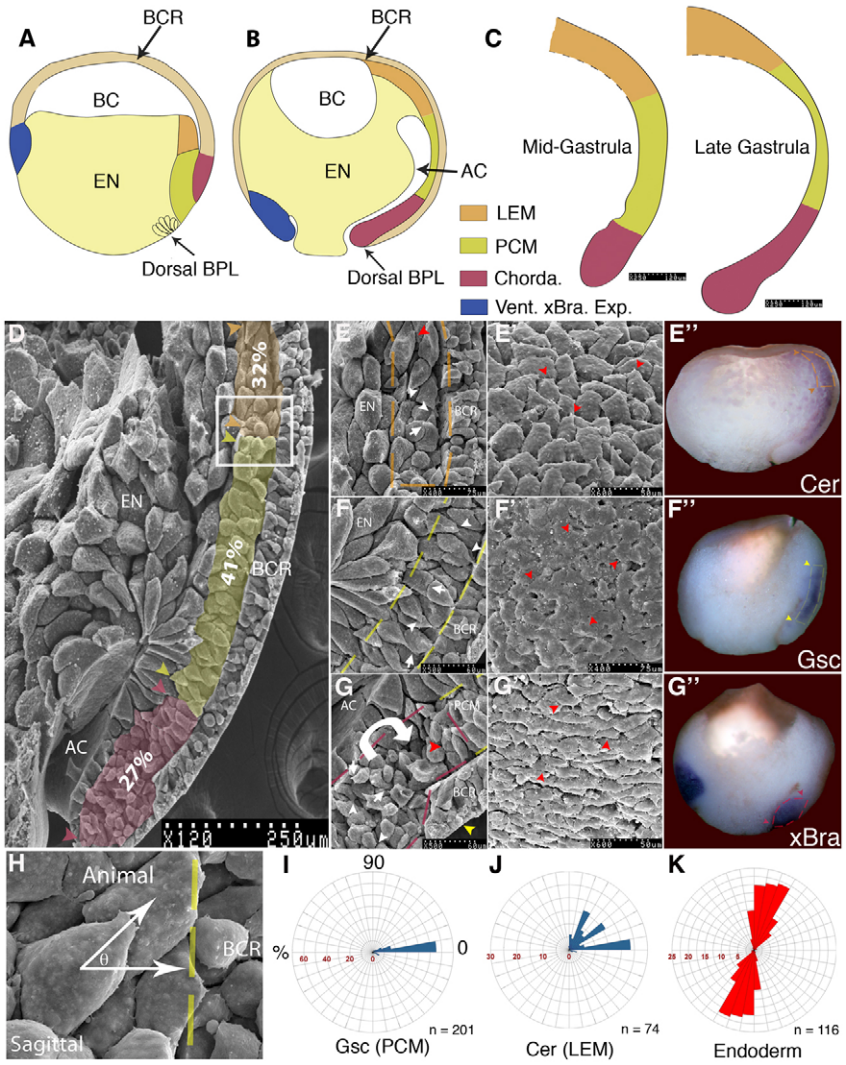

Fig. 1. Dorsal mesoderm during gastrulation. (**A**,**B**) Diagrams of (A) stage 10 (early gastrulation) and (B) stage 12 (late gastrulation); ventral Xbra expression is in blue. (**C**) Mesoderm regions at mid and late gastrulation, traced from SEM pictures. Scale bar: 120 µm. (**D**) SEM micrograph of sagittally fractured stage 11 embryo. Purple, chordamesoderm; yellow, PCM; orange, LEM. The percentage of the total mesoderm length occupied by each region is indicated. White box, transition between PCM and LEM. (**E-G**) High-magnification SEM images of (E) LEM, (F) PCM and (G) chordamesoderm from sagittally fractured stage 11 embryo; broken lines indicate boundaries of mesoderm regions. Cells extend protrusions in (white arrowheads) and out (white arrows) of the plane of the image. Red arrowhead in E indicates a cell with oblique orientation near the leading edge. Curved arrow in G indicates the direction of mesoderm internalization. Red arrowhead in G indicates a cell oriented perpendicular to the BCR at the anterior border of the region. (**E′-G′**) SEM images of (E′) LEM, (F′) PCM and (G′) chordamesoderm at stage 11, showing the surface previously in contact with the BCR. (E′) Red arrowheads indicate cells extending protrusions animally in a shingle arrangement. (F′) Red arrowheads indicate non-oriented cellular protrusions. (G′) Red arrowheads indicate bipolar cells in mediolateral orientation. (**E″-G″**) In situ hybridization for (E″) Cer, (F″) Gsc and (G″) Xbra; broken lines and arrowheads show region boundaries. (**H**) The angle (θ) between protrusion and the BCR as a measure of cell orientation. (**I-K**) Rose diagrams representing the percentage of cells extending protrusions (I,J), or the long axis (K) oriented with respect to BCR. 0° is towards the BCR, 90° toward the animal pole; *n*, number of cells; BCR, blastocoel roof; BPL, blastopore lip; BC, blastocoel; PCM, prechordal mesoderm; EN, endoderm; AC, archenteron; LEM, leading edge mesendoderm; Chorda, chordamesoderm.

radial intercalation by intercellular migration, and a massive insertion of deeper cells into the superficial layer of the PCM has indeed been observed (Winklbauer and Schurfeld, 1999). The measured rate of thinning (44 µm/2 hours) implies an average intercellular migration velocity of 0.4 µm/minute. Cell flattening probably contributes little to thinning; a single layer of cells flattened against the BCR is present throughout gastrulation (Fig. 1F, Fig. 2F).

Inhibition of PDGF signaling interferes with prechordal mesoderm radial intercalation, but not with chordamesoderm cell orientation

As PDGF-A is expressed in the BCR and the PDGFR-α in the mesoderm, we tested whether PDGF signaling orients PCM cell movement. Stage 11 embryos were treated with the cell-permeable PDGFR-α inhibitor AG1296 until DMSO-treated controls reached stage 12. Although the PCM became thinner in treated embryos, it consisted of two layers of cells oriented in parallel to the BCR (Fig. 2A-C,F-F′). By contrast, DMSO-treated control embryos had formed a single cell layer (Fig. 2B-C,F). In the AG1296-treated LEM, cells appeared more obliquely oriented compared with controls (Fig. 2G,G′). The post-involution chordamesoderm was unaffected by PDGF-A inhibition. As in controls, cells from AG1296-treated embryos were elongated perpendicular to the BCR (Fig. 2H,H′), and extended protrusions either towards or away from the BCR (Fig. 2D,E,H,H′; see Fig. S2G,H in the supplementary material). Furthermore, the layer indices of AG1296 and DMSO-treated embryos were similar (Fig. 2C). The results suggest that PDGF-A signaling is required to orient PCM cells towards the BCR and to prompt radial intercalation, but that radial orientation of the chordamesoderm is regulated by a different mechanism.

The short and long forms of PDGF-A are expressed in the BCR

sf-PDGF-A does not bind to extracellular matrix or the cell surface and may penetrate deep into tissues (Raines and Ross, 1992). Therefore, this isoform would be suited to control deep PCM cell movements. To determine which splice isoforms of PDFG-A are expressed in the BCR, we designed PCR primers flanking the putative spliced-out exon of the short isoform mRNA (Fig. 3A). The long isoform amplicon between the primers should be distinguishable from the short isoform by its larger size (Fig. 3A).

In RNA prepared from BCR, two bands corresponding to fragments of 240 bp (expected for long isoform) and 110 bp (short isoform) were observed (Fig. 3B). A third band of unknown identity was found at 225 bp (Fig. 3B); it may indicate a third isoform of PDGF-A similar to an intermediate short isoform found

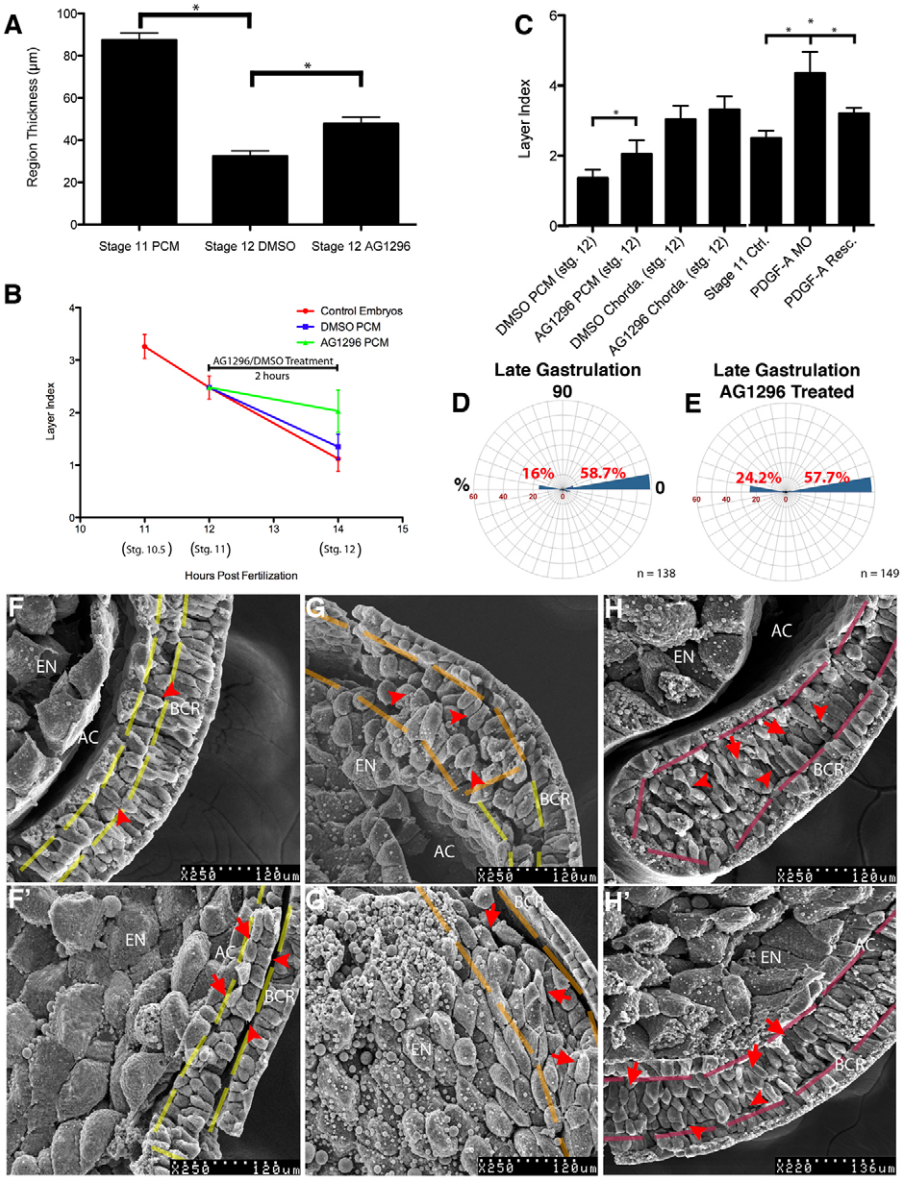

Fig. 2. PDGF-A inhibition disrupts PCM radial intercalation. (**A**) The PCM thins significantly ($P<0.0001$, $n=10$ embryos/stage) between stages 11 and 12; thinning is reduced upon AG1296 treatment ($P<0.0001$, $n=10$ embryos). (**B**) The change in layer index of PCM over time and following AG1296 treatment at stage 11. (**C**) The PCM layer index is significantly higher at stage 12 following AG1296 treatment ($P=0.0013$, $n=13$ embryos) or at stage 11 in PDGF-A MO-injected embryos ($P<0.0001$, $n=12$ embryos); chordamesoderm is unaffected ($P=0.0886$, $n=13$ embryos). (A-C) Error bars represent s.d., asterisks indicate significant results. (**D**,**E**) Orientation of chordamesoderm cells: BCR, 0°; n=number of cells. No significant difference between (D) controls and (E) AG1296-treated embryos ($P=0.9842$). (**F-H'**) Sagittally fractured stage 12 embryos treated with DMSO (F-H) or 10 µM AG1296 (F′-H′) 2 hours prior to fixation; broken lines indicate region boundaries. (F) Red arrowheads indicate PCM cells in a single layer in DMSO controls. (F′) Red arrowheads indicate superficial PCM cells in contact with the BCR; red arrows indicate a second layer of cells in AG1296-treated embryos. (G,G′) Red arrowheads indicate LEM cells oriented perpendicular to the BCR in controls (G) and obliquely oriented LEM cells in AG1296-treated embryos (G′). (H,H′) Red arrowheads indicate chordamesoderm cells extending protrusions towardsthe BCR; red arrows indicate cells extending protrusions toward the archenteron epithelium. BCR, blastocoel roof; EN, endoderm; AC, archenteron.

in chick (Horiuchi et al., 2001). The relative brightness of the 110 bp band (Fig. 3B), suggested that the short isoform is more abundant than the long form. BCR samples failed to show expression of PDGFR-α (Fig. 3B), in agreement with in situ hybridization data (Ataliotis et al., 1995).

We confirmed (Ataliotis et al., 1995) the lack of PDGF-A expression in mesodermal and vegetal cells, and the presence of PDGFR-α RNA in the mesoderm (Fig. 3B). Unexpectedly, vegetal cells also expressed PDGFR-α (Fig. 3B), which had not been detected by in situ hybridization. This could explain our finding that vegetal cells migrated directionally on conditioned substratum (Winklbauer and Nagel, 1991). However, as the vegetal cell mass also showed faint expression of Gsc and Xbra (Fig. 3B), we cannot exclude contamination by mesodermal cells.

sf-PDGF-A is an instructive cue required for radial orientation of prechordal mesoderm cells

To further analyze the role of PDGF-A in radial intercalation, an ATG morpholino antisense oligonucleotide (PDGF-A MO) that had been shown to inhibit PDGF-A signaling (Nagel et al., 2004) was used to knock down PDGF-A in embryos. Morphant embryos resembled those previously described (data not shown) (Ataiotis et al., 1995; Nagel et al., 2004). Mesoderm patterning is not affected by loss of PDGF-A signaling, as the mesoderm markers *gsc*, *Xbra* and *chordin* are expressed in the appropriate locations, and mesoderm derivatives, such as muscle and notochord, are present in respective embryos (Nagel et al., 2004; Ataliotis et al., 1995). We confirmed that *gsc* and *Xbra* were still expressed in morphant embryos (Fig. 4I,J), although the positions of the expression domains were slightly altered (compare Fig 1F″,G″ with Fig. 4I,J), consistent with a failure of mesoderm involution and archenteron elongation, as described previously (Nagel et al., 2009). Thus, although specification of mesodermal regions is not affected by an inhibition of PDGF-A signaling, morphogenetic movements are attenuated.

In morpholino-injected embryos, PCM and LEM cells were still elongated and unipolar (Fig. 4A). However, PCM cells were no longer strictly oriented towards the BCR (Fig. 4A,B), but at angles between 0° and 90°, i.e. between the original orientation and that of adjacent endodermal cells (Fig. 1I,K; Fig. 4A,B). Furthermore,

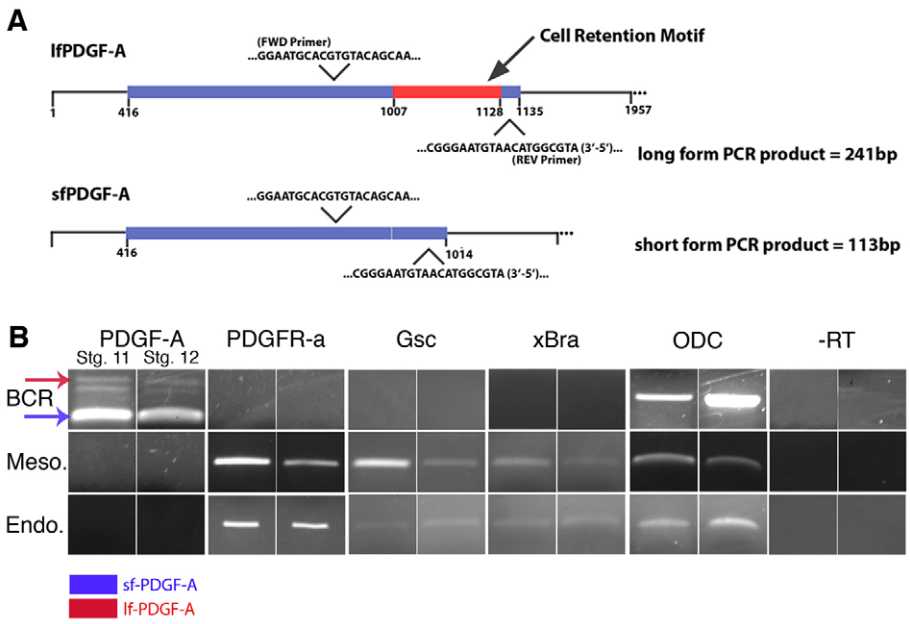

Fig. 3. Expression of PDGF-A isoforms and PDGFR-α in the gastrula.
(**A**) Diagram of long and short isoforms, primer pairs are indicated; red indicates a cell retention motif in the long isoform. (**B**) RT-PCR detection of PDGF-A isoforms and PDGFR-α in BCR, mesoderm (Meso) and endoderm (Endo). Red arrow indicates a 241 bp lf-PDGF-A product; blue arrow indicates a113 bp sf-PDGF-A product.

the layer index of PDGF-A MO-injected embryos was increased compared with controls (Fig. 2C), consistent with an inhibition of radial intercalation. LEM cells from morphant embryos were also more animally oriented compared with controls (Fig. 4B′). Injection with mRNA encoding the dominant-negative dnPDGF-A 1308 (Mercola et al., 1990) or a dominant-negative receptor, PDGFR-37 (Ataliotis et al., 1995), had similar effects on PCM and LEM cell orientation (Fig. 4C-D′; see Fig. S4A,D in the supplementary material). We conclude that the disruption of PCM and LEM cell orientation is due to an inhibition of PDGF-A signaling.

When morpholino-resistant mRNA encoding sf-PDGF-A was co-injected with PDGF-A MO, PCM cell orientation (Fig. 1D,F,I; Fig. 4E,F in the supplementary material) and layer index were rescued (Fig. 2C). LEM cell orientation was also affected by sf-PDGF-A: cells in this region were oriented even more radially compared with controls (Fig. 1E, Fig. 4F′). Involution movements and archenteron elongation were not rescued, however (data not shown). Overexpression in the BCR of sf-PDGF-A alone elicited a similarly increased BCR orientation of deep LEM cells, while it had no effect on the already oriented PCM cells (Fig. 4H,H′; see Fig. S4B in the supplementary material).

Morpholino-resistant lf-PDGF-A mRNA rescued neither PCM (Fig. 4G and data not shown) nor LEM cell orientation (Fig. 4G′), and overexpression of lf-PDGF-A in the BCR also had no effect on PCM orientation (data not shown). As similar lf-PDGF-A overexpression affected the orientation of cells in contact with the BCR (Nagel et al., 2004), the results suggest that although lf-PDGF-A is sensed by cells directly in contact with the BCR or its matrix, this signal is not relayed to the deep cells to affect their orientation.

If PDGF-A acted instructively as a guidance molecule, overexpression of sf-PDGF-A in the mesoderm should interfere with the ability of cells to detect an endogenous sf-PDGF-A gradient originating from the BCR. Indeed, in embryos expressing sf-PDGF-A in the mesoderm, cell orientation was similar to that in PDGF-A morphant embryos (Fig. 4K,K′; see Fig. S4C in the supplementary material). This loss of orientation could be rescued by co-injection of PDGF-A MO (MO non-resistant PDGF-A was used in these experiments) (see Fig. S4E,F,F′ in the supplementary material). This suggests that the short isoform of PDGF-A provides an instructive long-range guidance cue that is emitted by the BCR.

sf-PDGF-A is required for directional intercellular mesoderm migration in an explant system

To directly observe PDGF-A-dependent migration, dorsal mesoderm and endoderm, including the PCM was explanted and combined with BCR (Fig. 5A). This explant system preserves the endogenous tissue arrangement, and PCM cell movement should be directed towards the BCR. This was indeed observed (Fig. 5C). Moreover, although only cells at the explant surface can be filmed, which may move more easily between deeper cells and the coverslip than between lateral cells in this artificial situation, instances of radial intercalation were nevertheless observed (Fig. 5B,B′), consistent with the active migration of individual cells on each other's surface. When combined with PDGF-A MO-injected BCR, mesoderm cells did not move toward the BCR (compare Fig. 5D) and failed to intercalate (not shown). Although a tendency to move in parallel to the BCR was seen, migration was not massively redirected towards the animal pole, as could be inferred from the reorientation of cells seen in the SEM. At any rate, cells do not become permanently oriented when exposed to PDGF-A signaling, but the continuous presence of the signal is required to promote directed migration.

To test whether PDGF-A signaling is able to reorient cell migration, we developed a different explant system (Fig. 6A). The former posterior side of the PCM region of a mesoderm explant was brought into contact with the BCR. This array recapitulates the in vivo apposition of mesoderm and ectoderm while re-directing cell movements from radially to posteriorly. After 30 minutes, when explants had adjusted in response to the mechanical effects of apposition, cell movements were followed.

Cells exchanged neighbors while moving towards the BCR, again suggesting active directional migration of individual cells on cells deeper in the explant (Fig. 6B-E; see Movie 1 in the supplementary material). Deeper cells moved occasionally into view (Fig. 5D, turquoise cell) and also migrated towards the BCR.

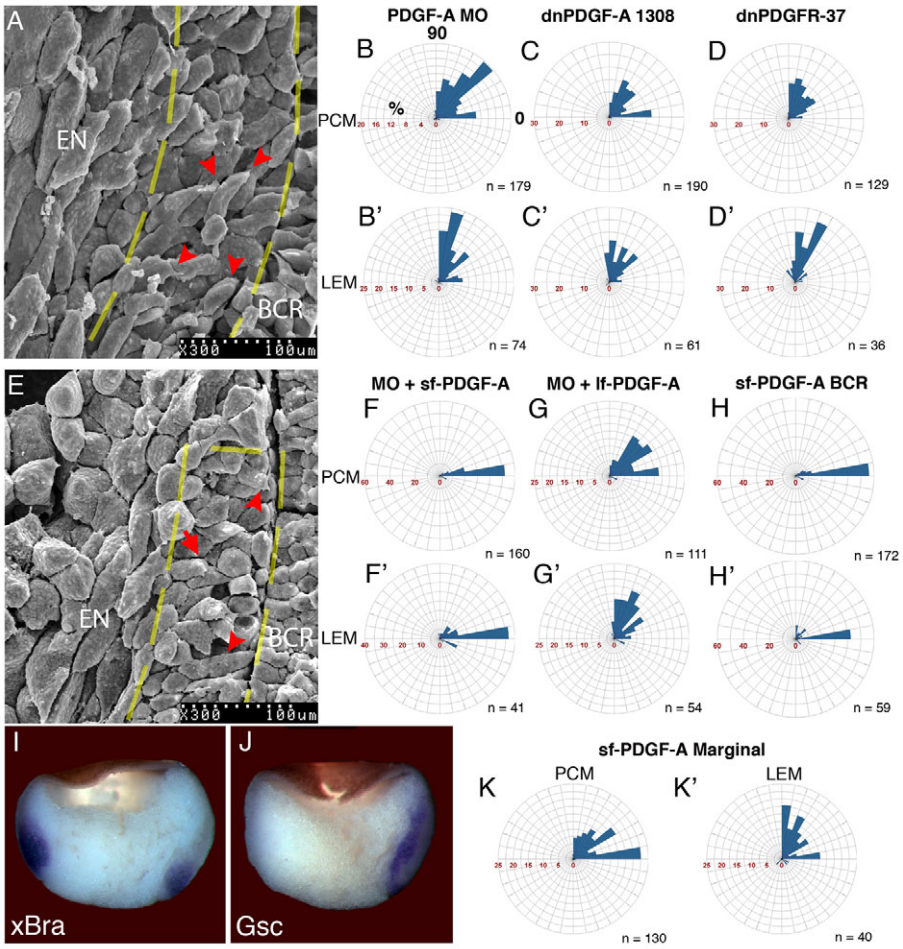

Fig. 4. sf-PDGF-A is required for radial orientation of PCM cells. (**A**) A sagittally fractured stage 11 embryo injected with 60 ng PDGF-A morpholino; cells are oriented parallel to the BCR (red arrowheads). The broken yellow lines indicate region boundaries. (**B-D′,F-H′**) Orientation of PCM cells (B-D,F-H) and LEM cells (B′-D′,F′-H′) from embryos injected with (B,B′) 60 ng PDGF-A morpholino, (C,C′) 1.6 ng of dominant-negative PDGF-A 1308 RNA, (D,D′) 400 pg of dominant-negative PDGFR-37 RNA, (F,F′) 60 ng PDGF-A MO + 800 pg sf-PDGF-A RNA, (G,G′) 60 ng PDGF-A MO + 800 pg lf-PDGF-A RNA or (H,H′) 800 pg sf-PDGF-A RNA. (**E**) Sagittally fractured stage 11 embryo co-injected with PDGF-A MO and sf-PDGF-A mRNA. Cells extend protrusions towards the BCR in (red arrowheads) and out (red arrows) of the plane of the image; the broken yellow line indicates the region boundary. (**I**,**J**) In situ hybridization for (I) Xbra and (J) Gsc from embryos injected with 60 ng PDGF-A MO. (**K**,**K′**) Orientation of cells from embryos injected with 400 pg of sf-PDGF-A mRNA in the mesoderm. n, number of cells per region; 0° and 90° correspond to BCR and animal pole, respectively. EN, endoderm; PCM, prechordal mesoderm; LEM, leading edge mesendoderm.

Although the BCR-mesoderm boundary was not perfectly blunt in cross-section, PCM cells did not use the BCR as a substratum to migrate over it (see Fig. S3D in the supplementary material), but apparently towards it.

Cell velocity was measured during consecutive 30-minute intervals (Fig. 6F-H). Directional movement of mesoderm cells within a five-cell diameter zone (zone R1) adjacent to the BCR was obvious 30 minutes after establishment of contact (Fig. 6F; see Movie 1 in the supplementary material); mesoderm explants lacking an attached BCR failed to show this effect (Fig. S3E). Directional movement continued over the next hour (Fig. 5F), at an average velocity of 0.8±0.03 μm/minute, i.e. similar to the in vivo rate. Cells located further from the BCR (zones R2 and R3; Fig. 6G,H) were motile but never moved directionally (Fig. 6G,H), probably being too far within the mesoderm to detect a chemotactic signal from the BCR.

Given that in the embryo, endodermal cells are only two to three cell lengths away from the BCR, but that the orienting signal can spread further, we suspected that endodermal cells may not respond to this signal. Indeed, endoderm cells in endoderm-BCR combinations did not migrate directionally (Fig. 7A).

We used the explant system to analyze the effect of PDGF-A knockdown on directional migration. Inner BCR injected with PDGF-A MO was placed in contact with normal mesoderm. Mesoderm cells were motile, but not moving directionally (Fig. 7B,C,C′; see Movie 2 in the supplementary material), until at 90 minutes some cells appeared to acquire directionality (Fig. 7B,C″; see Movie 2 in the supplementary material). This recovery may be due to an incomplete knockdown of PDGF-A. Co-injection of sf-PDGF-A rescued the effect of the PDGF-A MO (Fig. 7D-E″). We conclude that PDGF-A determines the direction of PCM cell movement, but that cells are able to migrate randomly in absence of PDGF-A signaling (Fig. 7B,C″; see Movie 2 in the supplementary material).

An instructive role for sf-PDGF-A signaling in directional migration

To determine whether the role of PDGF-A in the control of directionality is permissive or instructive, we performed gain-of-function experiments. We combined mesoderm with endoderm instead of BCR. As PDGF-A is normally not expressed in endoderm, mesoderm cells moved randomly (Fig. 8A-B″). Migration was also random when lf-PDGF-A was expressed in the endoderm by mRNA injection, confirming that this isoform has no long-range function (Fig. 8D). However, when sf-PDGF-A mRNA was injected instead, mesoderm cells moved directionally towards the endoderm (Fig. 8C; see Movie 3 in the supplementary material). To rule out the possibility that an unknown molecule from the endoderm acts as a guidance cue while PDGF-A is a permissive factor, we expressed sf-PDGF-A in the mesoderm. If secreted from the mesoderm in a uniform manner, sf-PDGF-A could act permissively for directional migration if additional factors were produced from the endoderm. However, mesoderm cells migrated randomly (Fig.

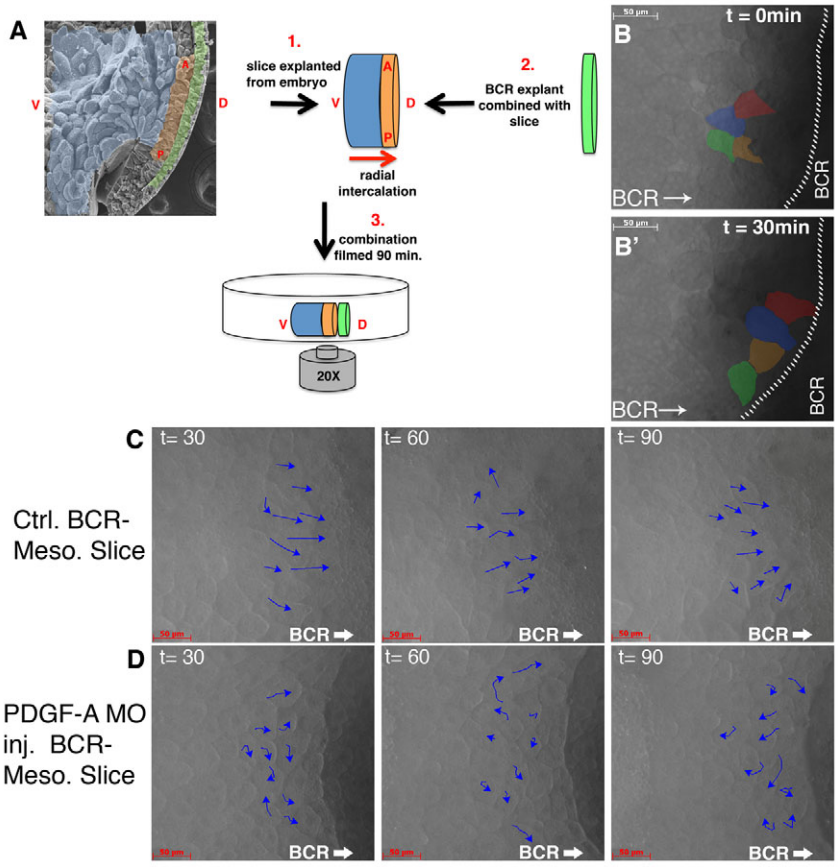

Fig. 5. PCM cell migration in vitro. (**A**) Explant system. (1) A slice of mesoderm and adjacent endoderm is combined with (2) explanted control or PDGF-A MO-injected BCR under a coverslip and (3) filmed to track mesoderm cell movements. Blue, endoderm; green, ectoderm; orange, mesoderm; red arrow shows the direction of cell intercalation; A, anterior; P, posterior; D, dorsal; V, ventral. (B-B′) Frames from timelapse recording. (**B**) Cell cluster at 0 minutes. (**B′**) Same cluster after 30 minutes; cells have intercalated at the mesoderm/BCR boundary (broken white line). (**C**,**D**) Cell tracks from explants combined with uninjected BCR (C) or BCR injected with 60 ng PDGF-A MO (D).

8E). This argues that the sf-PDGF-A instructively determines the orientation of PCM cells, and a localized source of sf-PDGF-A is sufficient to act as a directional cue.

DISCUSSION

We analyzed cell rearrangement in the prechordal mesoderm of *Xenopus*, and identified a mechanism for radial intercalation that depends on long-range PDGF-A signaling, intercellular migration of unipolar, oriented cells, and cell accumulation at the ectoderm-mesoderm boundary. Furthermore, we ascribe different functions – long-range and contact-dependent signaling – to short and long splice variants of PDGF-A, respectively.

A mechanism for radial cell intercalation in the prechordal mesoderm

Anterior mesoderm cells of the *Xenopus* gastrula extend protrusions in a unipolar fashion cell-autonomously, i.e. independent of external signals (Nagel et al., 2009). In the PCM, a sf-PDGF-A-mediated long-range signal reorients the protrusions of these unipolar cells from parallel to perpendicular to the BCR. The oriented protrusions are in contact with the cell bodies of adjacent cells. This suggests that cells use the surface of their neighbors and wedge between each other in an instance of intercellular migration, leading to radial intercalation and the gradual thinning of the PCM. The ability of the cells to migrate across adjacent cells towards a sf-PDGF-A source was directly demonstrated in vitro.

The PCM is separated from the ectodermal BCR by Brachet's cleft, a tissue boundary maintained by cycles of attachment and repulsion between ectoderm and mesoderm cells (Wacker et al., 2000) (N. Rohani, L. Canty, O. Luu, F. Fagotto and R.W., unpublished). The resulting dynamic adhesion between germ layers ensures that while the PCM cells can move across the BCR, they cannot penetrate into it despite being attracted by sf-PDGF-A. Lateral mobility on the BCR is essential for cells to efficiently wedge between each other and to accumulate at the boundary. The sf-PDGF-A signal potentially reaches about five cell lengths deep, but is only recognized by the PCM cells and not by endodermal cells deep to them. Therefore, given sufficient time, all PCM cells, and only these, will eventually arrive at the BCR to form a single layer. In summary, PCM thinning consists of a chemotactic reorientation of unipolar cells by an exogenous tissue, their intercellular migration and a boundary capture mechanism at Brachet's cleft.

A similar radial intercalation movement and consequent tissue spreading is observed during *Drosophila* gastrulation. Following invagination and an epithelial-to-mesechymal transition, a subset of deep mesodermal cells intercalate with more superficial cells that are in contact with the ectoderm (McMahon et al., 2010; McMahon et al., 2008; Murray and Saint, 2007). Radial intercalation of the deep cells depends on signaling by the FGF receptor *heartless* and its ligands Pyramus and Thisbe, which are all required for normal protrusion formation and intercalation (McMahon et al., 2010; Klingeisen et al., 2009; Murray and Saint, 2007). In our system, different isoforms of PDGF-A regulate both the intercalation of deep mesodermal cells and the directional migration of cells in contact with the BCR (current work and Nagel et al., 2004). Our preliminary results with the FGF receptor-specific inhibitor SU5402 suggested that FGF signaling plays no role in these processes (data not shown).

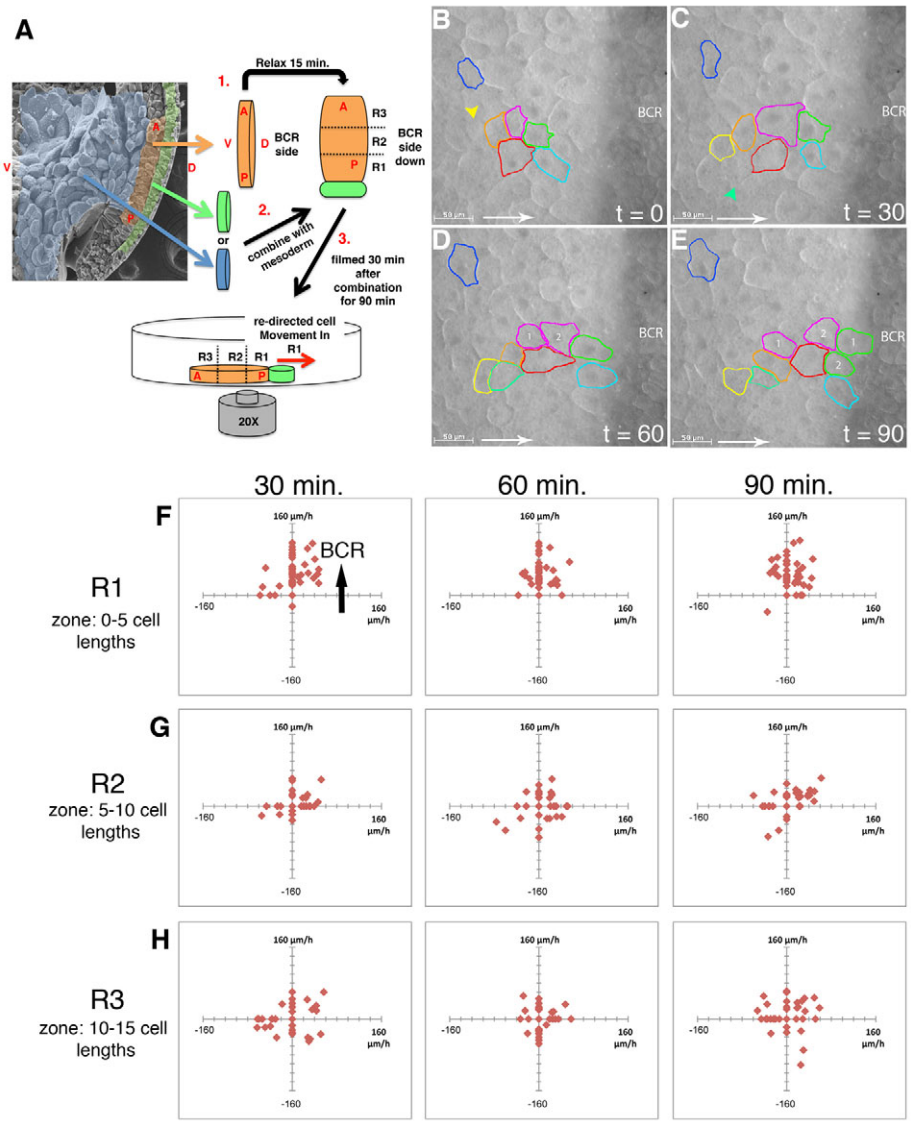

Fig. 6. PCM cells migrate directionally in vitro. (**A**) Explant system. (1,2) Mesoderm and endoderm or ectoderm are explanted, combined and left to relax for 15 minutes. BCR or endoderm are placed at the posterior, PCM-containing end of mesoderm explant, to force cells to reorient by 90° (from radially to posteriorly). Explant combinations (3) are filmed, and cell velocities measured. R1-R3, regions that are each five cell diameters wide. Blue, endoderm; green, ecotoderm; orange, mesoderm; red arrow, redirected cell movement; A, anterior; P, posterior; D, dorsal; V, ventral. (B-E) Frames from timelapse recording of a BCR-mesoderm explant. (**B**) Selected cells at 0 minutes. Yellow arrowhead indicates the position where a cell will emerge. (**C**) At 30 minutes, cells close to the BCR (green, light blue, purple and red) are moving towards the BCR. The position where a cell will emerge from below is marked by an arrowhead. (**D**) At 60 minutes, the light-blue cell has made contact with the BCR, the purple cell has divided and the turquoise cell has emerged. (**E**) At 90 minutes, the blue and green cells contact the BCR, and the green cell has divided. The dark-blue cell has remained at a constant distance from the BCR. (F-H) Velocity plots showing average velocities of 50 individual cells collected from five separate BCR-mesoderm explants. Positive *x*-axis is towards the BCR. (**F**) Cells in R1 migrate directionally. (**G**,**H**) Cells in R2 and R3 show random migration.

Distinct roles for long and short PDGF-A splice isoforms in cell orientation: contact-dependent and long-range signaling

Presence or absence of a cell-retention motif determines whether PDGF-A remains bound to the cell surface or ECM, or whether it is able to diffuse over larger distances (Andersson et al., 1994; Raines and Ross et al., 1992). Thus, PDGF-A molecules suited either for long-range signaling or for contact-dependent functions are generated by differential splicing (Andrae et al., 2008; Mercola et al., 1988). In *Xenopus*, the long and short isoforms serve indeed distinct functions in cell migration. The sf-PDGF-A orients PCM cells and attracts them to the BCR over a distance of several cell lengths. The lf-PDGF-A, on the other hand, associates with the extracellular matrix of the BCR by binding to proteoglycans or fibronectin (Smith et al., 2009; Nagel et al., 2004). With PDGFR-α being expressed in adjacent tissue, this creates a contact-dependent PDGF signaling mechanism where only mesoderm cells directly apposed to the BCR receive the signal. Consistent with this, the lf-PDGF-A has been linked to substrate-dependent guidance cues that direct the migration of anterior mesoderm on the BCR (Nagel et al., 2004).

The orienting signal from the BCR spreads about five cell layers deep into the mesoderm. As mesoderm does not express PDGF, a relay mechanism involving signal propagation by PDGF-stimulated PDGF release is excluded. Another possibility could be that PDGF-A triggers a relay mechanism based on other signaling molecules that would propagate the signal in the mesoderm and function as orienting cue. However, contact-dependent lf-PDGF-A is unable to orient distant cells in BCR rescue experiments and in endoderm gain-of-function assays, making such a relay mechanism unlikely. Instead, sf-PDGF-A may effectively diffuse into the mesoderm and form a classical chemoattractant gradient.

Unfortunately, the initial spreading of the signal could not be determined from the migratory response in explants, as irregular movements due to explant relaxation after explantation were superimposed over directed migration. After 30 minutes, approximately five cell rows were moving directionally, corresponding to a signal range of about 200 µm. The boundary of this oriented region advanced little during the next few hours. This would be consistent with a steady state gradient being formed within 1 hour, but also with a continuously expanding gradient

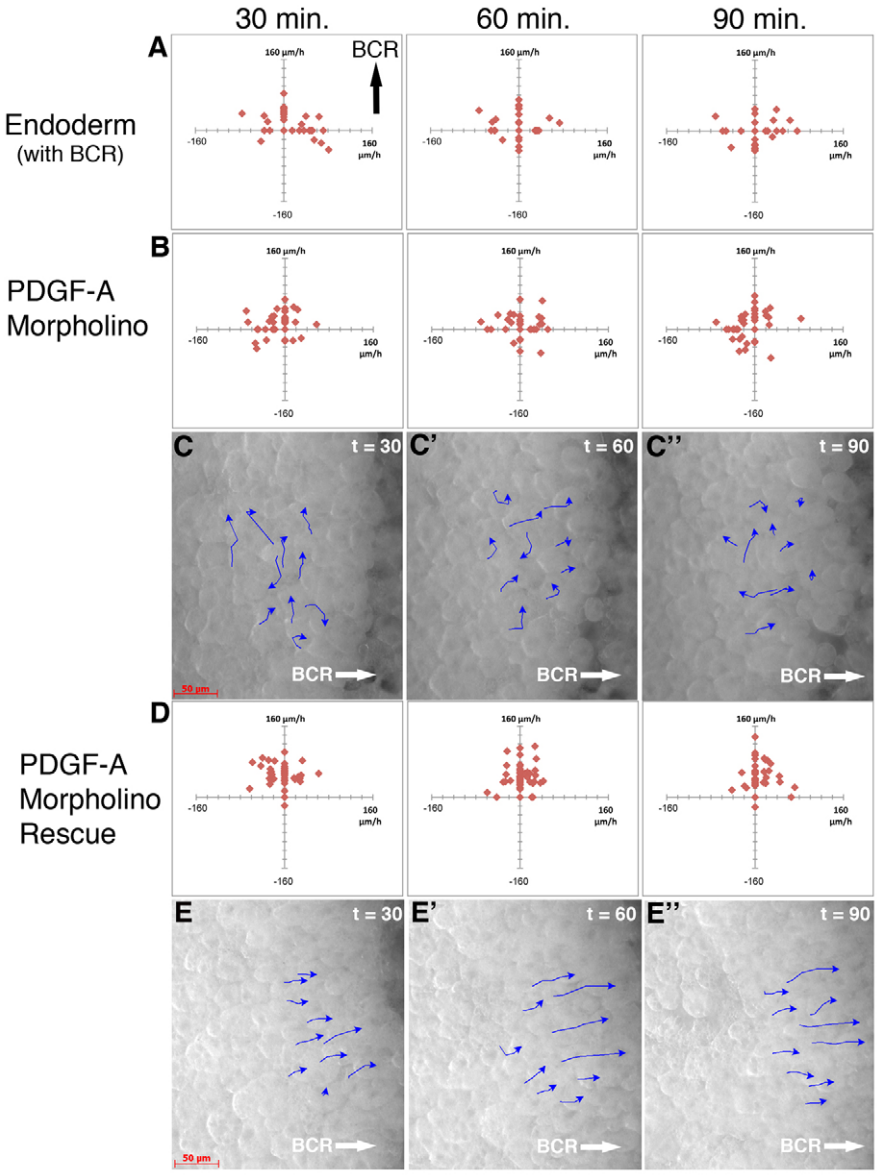

Fig. 7. sf-PDGF-A is required for directional migration of deep PCM cells. (**A**,**B**,**D**) Velocity plots, average velocities of 50 individual cells collected from five of each of the following combinations (attracting tissue/filmed tissue): (A) uninjected BCR/uninjected endoderm, (B) BCR injected with 60 ng PDGF-A MO/uninjected mesoderm, (D) BCR co-injected with 800 pg sf-PDGF-A mRNA and 60 ng PDGF-A morpholino/uninjected mesoderm. Positive *x*-axis is towards the BCR. (**C-C″**,**E-E″**) Tracks (blue arrows) of individual cells in mesodermal explant of B and D.

whose spreading velocity decreases exponentially. Compared with these length and time scales, the migration velocity of cells towards the source, about 20 µm/hour, is low, and will probably not significantly affect the gradient.

Formation of a steady state gradient involving localized production, apparent diffusion and degradation of a morphogen has been analyzed in the *Drosophila* wing disc (Entchev et al., 2000; Kicheva et al., 2007; Teleman and Cohen, 2000). A crucial parameter was the decay length, λ, the distance from the source at which morphogen concentration has decayed by a factor of 1/e. For Dpp-GFP in the wing disc:

$$\lambda = \sqrt{\frac{D}{k}} ,$$

where D is the diffusion coefficient and k is the degradation rate, was found to be 20 µm. Since the size of the PDGF-A dimer is similar to Dpp-GFP, D may also be similar. If we assume that the gradient is read by mesoderm cells to a distance of 2λ=200 µm (to 20% of the concentration at the origin), a stable gradient of the required length could be formed if the degradation rate for PDGF in mesoderm were 25 times lower than that of Dpp in the wing disc. Moreover, in the *Xenopus* BCR, an extracellular activin gradient was established experimentally across a distance of over 400 µm within 1 hour (Hagemann et al., 2009). Altogether, the length and time scales of induced directional migration in our assay are consistent with a gradient of diffusible PDGF.

Roles for PDGF-A and PDGFR-α have been identified during early development of zebrafish, chick and mouse (Yang et al., 2008; Orr-Urtreger et al., 1992; Soriano, 1997; Montero et al., 2003), but it is not known which isoforms of PDGF-A are involved, and whether boundary effects or long-range signals are employed. In addition, PDGF-A has functions other than cell orientation in the embryo. It prevents apoptosis in the mesoderm of *Xenopus* (Van Stry et al., 2004; Van Stry et al., 2005), and regulates N-cadherin expression in the chick (Yang et al., 2008). In zebrafish, PDGF-A is part of a signaling pathway involving PI3K and PKB, which stimulates the formation of PCM cell protrusions during gastrulation (Montero et al., 2003).

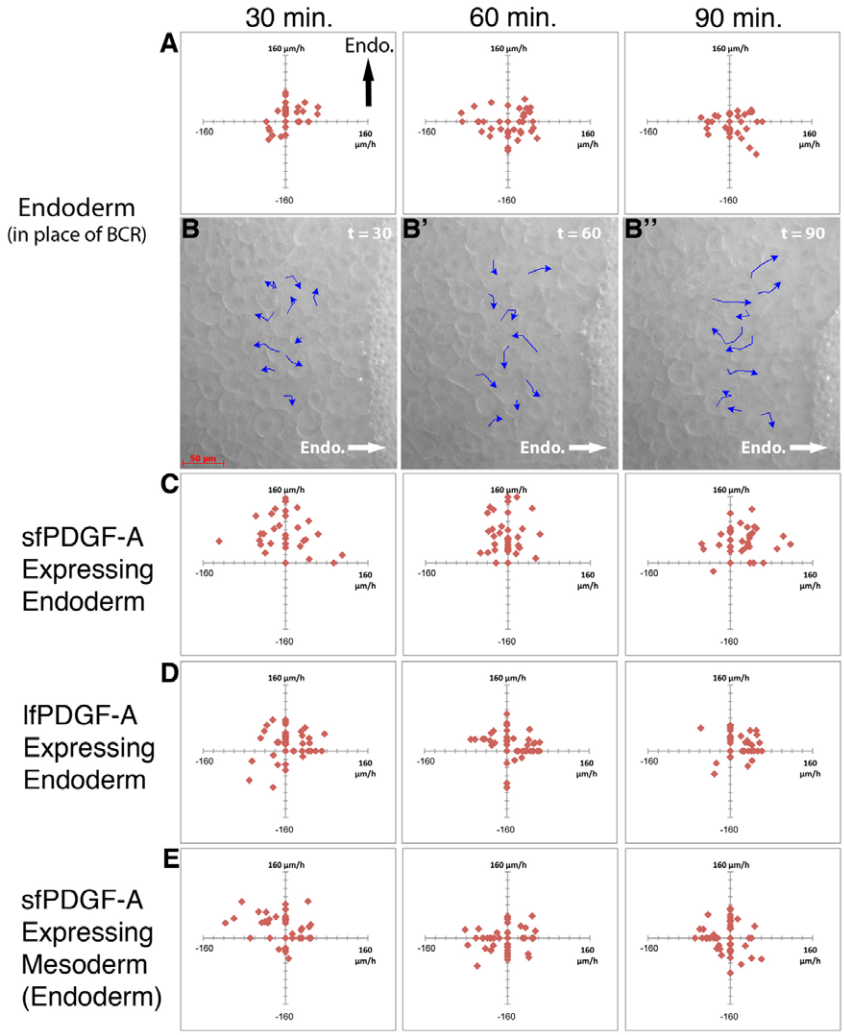

Fig. 8. sf-PDGF-A is an instructive cue for PCM directional migration. (**A**,**C-E**) Velocity plots showing velocities of 50 individual PCM cells from five of each of the following explant combinations (attracting tissue/filmed tissue): (A) uninjected endoderm/mesoderm, (C) endoderm injected with 400 pg sf-PDGF RNA/uninjected mesoderm, (D) endoderm injected with 400 pg lfPDGF-A/uninjected mesoderm and (E) uninjected endoderm/mesoderm injected with 400 pg sf-PDGF-A RNA. Positive *x*-axis is toward the endoderm. (**B-B″**) Tracks (blue arrows) of PCM cells from uninjected endoderm/uninjected mesoderm combination. Endo, endoderm.

Patterns of cell orientation and radial intercalation in *Xenopus* gastrulation

In the chordamesoderm, mediolateral intercalation of bipolar cells drives convergent extension (Shih and Keller, 1992; Wallingford et al., 2000; Keller, 2002), but cells in this region also intercalate radially (Wilson and Keller, 1991), and are elongated correspondingly (Keller and Schoenwolf, 1977). Although these cells seem to be unipolar, protrusions can point either towards or away from the BCR, suggesting a bidirectional mode of radial intercalation where cells can move in either one or the other direction. Thinning of the region during gastrulation is only moderate (Fig. 1C). The cues for this radial intercalation are not known. It does not depend on PDGF signaling, and in explants it occurs tissue-autonomously in the absence of BCR interaction (Wilson and Keller, 1991).

In the PCM, cells are all strictly oriented towards the BCR, engaging in a mode of radial intercalation that may therefore be termed unidirectional. Towards the LEM, orientation grades into an oblique pattern. The LEM translocates as a whole in the direction of the animal pole (Winklbauer and Nagel, 1991; Nagel et al., 2004) without intercalating radially (Winklbauer and Schurfeld, 1999) and without thinning (Fig. 1C). Both in PCM and LEM, orientation is influenced by sf-PDGF-A. If signaling is diminished, PCM cells assume an orientation characteristic of the LEM, and conversely, when sf-PDGF-A is overexpressed, LEM cells become radially oriented, similar to the PCM. A lower sensitivity towards the PDGF signal in the LEM, consistent with the reduced expression of PDGFR-α in this region (Ataliotis et al., 1995), could explain the difference in the degree of orientation. However, the matrix-bound lf-PDGF-A is still able to promote the animally directed orientation of LEM cells in contact with the BCR (Nagel et al., 2004).

Several observations suggest that the dorsal pattern of cell orientation continues laterally and ventrally. Bidirectional orientation extends laterally into the presomitic mesoderm, which takes part in convergent extension (E.W.D. and R.W., unpublished). Unidirectional radial and oblique orientation is seen in ventral mesoderm (Ibrahim and Winklbauer, 2001). We propose that the whole mesoderm can be subdivided into a PDGF-insensitive bidirectionally oriented region, and a PDGF-sensitive unidirectional population. The former would comprise the converging and extending mesoderm, and the latter both the LEM with its oblique orientation, and an intermediate region where cells point straight towards the BCR.

Unidirectional radial intercalation in the PCM and corresponding lateral and ventral regions is associated with strong tissue spreading. In fact, this zone has to expand most as the mesoderm moves animally, given the spherical geometry of the gastrula (Keller and Tibbetts, 1989; Winklbauer and Schurfeld, 1999; Ibrahim and Winklbauer, 2001). Anterior to the spreading region,

the LEM converges in the process of mantle closure (Davidson et al., 2002), and behind it, convergence of the posterior mesoderm closes the blastopore (Keller et al., 2003; Keller and Shook, 2008). Importantly, spreading depends on an interaction with the BCR, but not with its FN matrix (Winklbauer and Schurfeld, 1999). It is due to an attraction of cells by the BCR, and is not driven by FN-dependent migration across the BCR surface.

The endodermal vegetal cell mass is not responsive to the long-range sf-PDGF-A signal. However, cells express PDGFR-α, and endodermal explants migrate directionally on BCR-conditioned substratum (Winklbauer and Nagel, 1991), consistent with an ability to recognize lf-PDGF-A. In the embryo, vegetal cells are elongated in an animal-vegetal direction, i.e. in parallel and not perpendicular to the BCR, fitting to the vegetal rotation movement in which these cells are engaged (Winklbauer and Schurfeld, 1999). In the absence of a sf-PDGF-A signal, PCM cells take on a similar orientation. This suggests that in mesoderm and vegetal endoderm, basic cell orientation is along the animal/vegetal axis. As mesoderm cells respond to PDGF, they are reoriented toward the BCR, to a degree that depends on the strength of this competing signal.

Acknowledgements
This work was supported by a Canadian Institutes of Health Research grant (MOP-53075) to R.W. We thank K. Symes, E. De Robertis and H. Steinbeisser for constructs, A. Bruce, T. Harris and M. Nagel for critical reading of the manuscript, and all members of the Winklbauer lab for helpful suggestions and criticism.

Competing interests statement
The authors declare no competing financial interests.

Supplementary material
Supplementary material for this article is available at
http://dev.biologists.org/lookup/suppl/doi:10.1242/dev.056903/-/DC1

References
Andersson, M., Ostman, A., Westermark, B. and Heldin, C. (1994). Characterization of the retention motif in the C-terminal part of the long splice form of platelet-derived growth factor A-chain. *J. Biol. Chem.* **269**, 926-930.
Andrae, J., Gallini, R. and Betsholtz, C. (2008). Role of platelet-derived growth factors in physiology and medicine. *Genes Dev.* **22**, 1276-1312.
Ataliotis, P., Symes, K., Chou, M., Ho, L. and Mercola, M. (1995). PDGF signalling is required for gastrulation of Xenopus Laevis. *Development* **121**, 3099-3110.
Bouwmeester, T., Kim, S., Sasai, Y., Lu, B. and De Robertis, E. (1996). Cerberus is a head-inducing secreted factor expressed in the anterior endoderm of Spemann's organizer. *Nature* **382**, 595-601.
Cho, K., Blumberg, B., Steinbeisser, H. and De Robertis, E. (1991). Molecular nature of Spemann's organizer: the role of the Xenopus homeobox gene goosecoid. *Cell* **67**, 1111-1120.
Davidson, L., Hoffstrom, B., Keller, R. and DeSimone, D. (2002). Mesendoderm extension and mantle closure in Xenopus laevis gastrulation: combined roles for integrin α5β1, fibronectin, and tissue geometry. *Dev. Biol.* **242**, 109-129.
Entchev, E. V., Schwabedissen, A. and Gonzalez-Gaitan, M. (2000). Gradient formation of the TGF-β homolog Dpp. *Cell* **103**, 981-991.
Hagemann, A., Xu, X., Nentwich, O., Hyvonen, M. and Smith, J. (2009). Rab5-mediated endocytosis of Activin is not required for gene activation or long-range signalling in Xenopus. *Development* **136**, 2803-2813.
Harland, R. (1991). In situ hybridization: an improved whole-mount method for Xenopus embryos. *Methods Cell Biol.* **36**, 685-695.
Horiuchi, H., Inoue, T., Furusawa, S. and Matsuda, H. (2001). Characterization and expression of three forms of cDNA encoding chicken platelet-derived growth factor-A chain. *Gene* **272**, 181-190.
Ibrahim, H. and Winklbauer, R. (2001). Mechanisms of mesendoderm internalization in the Xenopus gastrula: lessons from the ventral side. *Dev. Biol.* **240**, 108-122.
Keller, R. (1980). The cellular basis of epiboly: an SEM study of deep-cell rearrangement during gastrulation in Xenopus Laevis. *J. Embryol. Exp. Morphol.* **60**, 201-234.
Keller, R. (2002). Shaping the vertebrate body plan by polarized embryonic cell movements. *Science* **298**, 1950-1954.
Keller, R. and Schoenwolf, G. (1977). An SEM study of cellular morphology, contact and arrangement, as related to gastrulation in *Xenopus laevis*. *Roux's Arch. Dev. Biol.* **182**, 165-186.
Keller, R. and Tibbetts, P. (1989). Mediolateral cell intercalation in the dorsal, axial mesoderm of Xenopus Laevis. *Dev. Biol.* **131**, 539-549.
Keller, R. and Shook, D. (2008). Dynamic determinations: patterning the cell behaviours that close the amphibian blastopore. *Phil. Trans. R. Soc. B* **363**, 1317-1332.
Keller, R., Davidson, L. and Shook, D. (2003). How we are shaped: the biomechanics of gastrulation. *Differentiation* **71**, 171-205.
Kicheva, A., Pantazis, P., Bollenbach, T., Kalaidzidis, Y., Bittig, T., Julicher, F. and Gonzalez-Gaitan, M. (2007). Kinetics of morphogen gradient formation. *Science* **315**, 521-525.
Klingeisen, A., Clark, I. B., Gryzik, T. and Muller, H.-A. J. (2009). Differential and overlapping functions of two closely related Drosophila FGF8-like growth factors in mesoderm development. *Development* **136**, 2393-2402.
Luu, O., Nagel, M., Wacker, S., Lemaire, P. and Winklbauer, R. (2008). Control of gastrula cell motility by the Goosecoid/Mix.1/Siamois network: basic patterns and paradoxical effects. *Dev. Dyn.* **237**, 1307-1320.
Marsden, M. and DeSimone, D. (2001). Regulation of cell polarity, radial intercalation and epiboly in Xenopus: novel roles for integrin and fibronectin. *Development* **128**, 3635-3647.
McMahon, A., Supatto, W., Fraser, S. and Stathopoulos, A. (2008). Dynamic analyses of Drosophila gastrulation provide insight into collective cell migration. *Science* **322**, 1546-1550.
McMahon, A., Reeves, G., Supatto, W. and Stathopoulos, A. (2010). Mesoderm migration in Drosophila is a multi-step process requiring FGF signaling and integrin activity. *Development* **137**, 2167-2175.
Mercola, M., Deininger, P., Shamah, S., Porter, J., Wang, C. and Stiles, C. (1990). Dominant-negative mutants of a platelet-derived growth factor gene. *Genes Dev.* **4**, 2333-2341.
Mercola, M., Melton, D. and Stiles, C. (1988). Platelet-derived growth factor a chain is maternally encoded in Xenopus embryos. *Science* **241**, 1223-1225.
Montero, J., Kilian, B., Chan, J., Bayliss, P. and Heisenberg, C. (2003). Phosphoinositide 3-kinase is required for process outgrowth and cell polarization of gastrulating mesendodermal cells. *Curr. Biol.* **13**, 1279-1289.
Murray, M. and Saint, R. (2007). Photoactivatable GFP resolves Drosophila mesoderm migration behaviour. *Development* **134**, 3975-3983.
Nagel, M., Tahinci, E., Symes, K. and Winklbauer, R. (2004). Guidance of mesoderm cell migration in the Xenopus gastrula requires PDGF signaling. *Development* **131**, 2727-2736.
Nagel, M., Luu, O., Bisson, N., Macanovic, B., Moss, T. and Winklbauer, R. (2009). Role of p21-activated kinase in cell polarity and directional mesendoderm migration in the Xenopus gastrula. *Dev. Dyn.* **238**, 1709-1726.
Nieuwkoop, P. D. and Faber, J. (1967). *Normal Table of* Xenopus laevis *(Daudin)*. Amsterdam: North-Holland.
Orr-Urtreger, A. and Lonai, P. (1992). Platelet-derived growth factor-A and its receptor are expressed in separate, but adjacent cell layers of the mouse embryo. *Development* **115**, 1045-1058.
Raines, E. and Ross, R. (1992). Compartmentalization of PDGF on extracellular binding sites dependent on exon-6-encoded sequences. *J. Cell Biol.* **116**, 533-543.
Shih, J. and Keller, R. (1992). Cell motility driving mediolateral intercalation in explants of Xenopus laevis. *Development* **116**, 901-914.
Smith, E., Mitsi, M., Nugent, M. and Symes, K. (2009). PDGF-A interactions with fibronectin reveal a critical role for heparan sulfate in directed cell migration during Xenopus gastrulation. *Proc. Natl. Acad. Sci. USA* **106**, 21683-21688.
Soriano, P. (1997). The PDGF alpha receptor is required for neural crest cell development and for normal patterning of the somites. *Development* **124**, 2691-2700.
Teleman, A. A. and Cohen, S. M. (2000), Dpp gradient formation in the *Drosophila* wing imaginal disc. *Cell* **103**, 971-980.
Van Stry, M., McLaughlin, K., Ataliotis, P. and Symes, K. (2004). The mitochondrial-apoptotic pathway is triggered in Xenopus mesoderm cells deprived of PDGF receptor signaling during gastrulation. *Dev. Biol.* **268**, 232-242.
Van Stry, M., Kazlauskas, A., Schreiber, S. and Symes, K. (2005). Distinct effectors of platelet-derived growth factor receptor-alpha signaling are required for cell survival during embryogenesis. *Proc. Natl. Acad. Sci. USA* **102**, 8233-8238.
Wacker, S., Grimm, K., Joos, T. and Winklbauer, R. (2000). Development and conrol of tissue separation at gastrulation in Xenopus. *Dev. Biol.* **224**, 428-439.
Wallingford, J., Rowing, B., Vogeli, K., Rothbacher, U., Fraser, S. and Harland, R. (2000). Dishevelled controls cell polarity during Xenopus gastrulation. *Nature* **405**, 81-85.
Wilkinson, D., Bhatt, S. and Herrmann, B. (1990). Expression pattern of the mouse T gene and its role in mesoderm formation. *Nature* **343**, 657-659.
Wilson, P. and Keller, R. (1991). Cell rearrangement during gastrulation of Xenopus: direct observation of cultured explants. *Development* **112**, 289-300.
Winklbauer, R. and Nagel, M. (1991). Directional mesoderm cell migration in the Xenopus gastrula. *Dev. Biol.* **148**, 573-589.
Winklbauer, R. and Schurfeld, M. (1999). Vegetal rotation, a new gastrulation movement involved in the internalization of the mesoderm and endoderm in Xenopus. *Development* **126**, 3703-3713.
Yang, X., Chrisman, H. and Weijer, C. (2008). PDGF signalling controls the migration of mesoderm cells during chick gastrulation by regulating N-Cadherin expression. *Development* **135**, 3521-3530.